

Living Anionic Polymerization of 4-Vinyltriphenylamine for Synthesis of Novel Block Copolymers Containing Low-Polydisperse Poly(4-vinyltriphenylamine) and Regioregular Poly(3-hexylthiophene) Segments

Tomoya Higashihara* and Mitsuru Ueda

Department of Organic and Polymeric Materials, Graduate School of Science and Engineering,
Tokyo Institute of Technology 2-12-1-H-120, O-okayama, Meguro-Ku, Tokyo 152-8552, Japan

Received July 24, 2009; Revised Manuscript Received September 2, 2009

ABSTRACT: We have developed a living anionic polymerization of 4-vinyltriphenylamine (VTPA) in *tert*-butylbenzene at 25 °C or tetrahydrofuran at –78 °C initiated with *sec*-butyllithium in the absence of any additives based on a high-vacuum (10^{-6} Torr) technique. Lithium naphthalenide could also initiate the polymerization of VTPA to generate difunctional living PVTPA. The molecular weights of poly(VTPA) (PVTPA) were proportionally increased up to around 30 K by increasing the feed ratio of VTPA to the initiator, while keeping very low polydispersities (PDIs) of less than 1.1. A new series of block copolymers, PVTPA-*b*-poly(methyl methacrylate) and polystyrene (PS)-*b*-PVTPA-*b*-PS, have been successfully synthesized by exploiting the living nature of PVTPA. We were also successful in synthesizing novel and optoelectronically active coil–rod–coil triblock copolymers comprised of regioregular poly(3-hexylthiophene) (P3HT) and PVTPA segments. Their characterization as well as thermal and optical properties have been investigated. Furthermore, the self-assemble behavior of the block copolymers displaying periodic nanostructures has been confirmed by atomic force microscopy and transmission electron microscopy.

Introduction

Poly(4-vinyltriphenylamine) (PVTPA) contains pendant triphenylamine chromophores and possesses excellent hole-transporting characteristics. Indeed, the utility of PVTPA in the field of organic light-emitting diodes (OLEDs) has been described.^{1,2} A number of studies have been made for the synthesis of well-defined poly(4-vinyltriphenylamine) (PVTPA) with predictable number-average molecular weights (M_n s) and low polydispersity indices (PDIs) based on anionic^{3,4} and controlled radical polymerization.^{3,5–8} However, high- M_n PVTPA of more than 10K have never been prepared by anionic polymerization. Although it was possible to synthesize high- M_n PVTPA based on radical polymerization, the PDIs were rather broad ($PDI > 1.2$).^{5–8} Se et al. reported a living anionic polymerization of *N,N*-dimethyl-4-vinylphenylamine, whose structure is similar to that of 4-vinyltriphenylamine (VTPA), to afford well-defined poly(*N,N*-dimethyl-4-vinylphenylamine) with an M_n value of more than 70K and low PDI (< 1.1) by using cumyl cesium as the initiator in THF at –78 °C under a high vacuum (10^{-6} Torr) condition.⁹ Recently, Natori et al. described the living anionic polymerization of VTPA initiated with *tert*-butyllithium in the presence of, *N,N,N',N'*-tetramethylethylenediamine (TMEDA), in toluene at room temperature under dry argon.¹⁰ Although the molecular weights increased up to around 56K, unfortunately, the PDIs were not very low ($PDI = 1.1–1.27$) as a living anionic polymerization system. There has never been a report on living anionic polymerization of VTPA with reasonably high M_n values and low PDIs of less than 1.1. Therefore, we were motivated to develop a simple, additive-free living system of the anionic polymerization of VTPA to prepare a low-polydisperse PVTPA ($PDI < 1.1$).

On the other hand, regioregular poly(3-alkylthiophene) is important high-performance material due to its high charge mobility, high solubility, and synthetic facility. These superior characteristics are readily accessible for optoelectronic device applications such as organic field effect transistors¹¹ and photovoltaic cells.¹² Recent efforts in the development of quasi-living Grignard metathesis (GRIM) polymerization^{13,14} currently open further molecular designs and modifications of π -conjugated polymer architecture combining dual- or multi-functions. Much attention has also been paid to poly(3-alkylthiophene)-based block copolymers^{13,15–25} because hierarchical nanostructures are generally derived from self-assembly so as to minimize contact energy between dissimilar polymer domains.

Recently, our group developed a facile approach starting from α,ω -difunctional P3HT with 1,1-diphenylethylene moieties (DPE–P3HT–DPE) to synthesize a novel series of ABA type coil–rod–coil triblock copolymers, PS-*b*-P3HT-*b*-PS²⁶ and PMMA-*b*-P3HT-*b*-PMMA.²⁷ Since these block copolymers contain insulating segments, their electronic performance is probably limited. Therefore, the introduction of optoelectronically active coil segments into P3HT-based block copolymers is highly desired.

Herein we describe the living anionic polymerization of VTPA and its application to the first synthesis of well-defined coil–rod–coil triblock copolymers consisting of low-polydisperse PVTPA and regioregular P3HT segments, PVTPA-*b*-P3HT-*b*-PVTPA. The target block may be one of candidates as better hole-transporting material than PS-*b*-P3HT-*b*-PS or PMMA-*b*-P3HT-*b*-PMMA. Facile, additive-free living anionic polymerization of VTPA as well as the synthesis, characterization, thermal and optical properties, and self-assembly behavior of PVTPA-*b*-P3HT-*b*-PVTPA are particularly focused in this article. In order to confirm the living nature of anionic

*Corresponding author: Tel +81-3-5734-2126, Fax +81-3-5734-2126,
E-mail thigashihara@polymer.titech.ac.jp.

polymerization of VTPA prior to the synthesis of PVTPA-*b*-P3HT-*b*-PVTPA, another series of new block copolymers, PS-*b*-PVTPA-*b*-PS triblock and PVTPA-*b*-PMMA diblock copolymers, were also synthesized.

Experimental Section

Materials. All chemicals (>98% purities) were purchased from Aldrich, Japan, and used as received unless otherwise noted. Tetrahydrofuran (THF) (99%, Mitsubishi Chemical Co., Ltd.) was refluxed over sodium wire for 12 h and then distilled from lithium aluminum hydride under nitrogen. It was finally distilled from its sodium naphthalenide solution on a high-vacuum line (10^{-6} Torr). *tert*-Butylbenzene was washed with concentrated sulfuric acid, water, 10% NaOH(aq), and water. It was dried over calcium chloride and phosphorus pentoxide and then distilled from 1,1-diphenylhexyllithium on the vacuum line. 1,1-Diphenylethylene (DPE) was distilled from calcium hydride under reduced pressure and then distilled from 1,1-diphenylhexyllithium. Lithium chloride (LiCl) was dried under high vacuum (10^{-6} Torr) at 100 °C for 2 days and titrated with a THF solution of potassium naphthalenide. *sec*-BuLi was used after diluting with dry heptane. Lithium naphthalenide (Li-Naph) was prepared by the reaction of lithium with naphthalene. MMA (>99%) was distilled from calcium hydride and trioctylaluminum on the vacuum line. Styrene was distilled from calcium hydride and finally distilled from dibutylmagnesium (ca. 5 mol %) on the vacuum line. VTPA² and DPE–P3HT–DPE²⁶ were synthesized according to the previous paper.

Living Anionic Polymerization of 4-Vinyltriphenylamine. All polymerizations were carried out under high-vacuum conditions (10^{-6} Torr) in sealed glass reactors with break-seals. The reactors were always prewashed with the initiator solutions after being sealed off from the vacuum line. *sec*-BuLi-initiated polymerization of VTPA was carried out in *tert*-butylbenzene at 25 °C for 24 h or in THF at –78 °C for 12 h. The polymerization of VTPA with Li-Naph was carried out in THF at –78 °C for 12 h.

Synthesis of PVTPA-*b*-PMMA. To *sec*-BuLi (0.0530 mmol) was added a THF solution (7.20 mL) of VTPA (1.89 mmol) at –78 °C. Then, the polymerization system was allowed to stand at –78 °C for 12 h, followed by the addition of a THF solution (2.50 mL) of DPE (0.0795 mmol) and a THF solution (4.56 mmol) of LiCl (0.265 mmol). After 2 h for the complete DPE capping, a THF solution (8.50 mL) of MMA (8.04 mmol) was added at once with vigorous stirring set at 700 rpm. After stirring for 30 min, degassed methanol was added, and the solution was poured into a large amount of methanol (200 mL) to precipitate the polymer. Yield: 1.28 g (97%). M_n (GPC-RALLS) = 24 000, M_n (¹H NMR) = 25 500, PDI = 1.04.

Synthesis of PS-*b*-PVTPA-*b*-PS. To a THF solution (2.01 mL) of Li-Naph (0.0558 mmol) was added a THF solution (7.35 mL) of VTPA (1.91 mmol) at –78 °C. Then, the polymerization system was allowed to stand at –78 °C for 12 h. Then, a THF solution (5.11 mL) of styrene (5.12 mmol) was added at once. After stirring at –78 °C for 30 min, degassed methanol was added, and the solution was poured into a large amount of methanol (200 mL) to precipitate the polymer. Yield: 1.04 g (96%). M_n (GPC-RALLS) = 38 000, M_n (¹H NMR) = 38 600, PDI = 1.07.

Synthesis of PVTPA-*b*-P3HT-*b*-PVTPA. In a typical experiment (run 10), to *sec*-BuLi (0.038 mmol) was added a THF solution (4.20 mL) of VTPA (1.39 mmol) at –78 °C. Then, the polymerization was allowed to stand at –78 °C for 12 h, followed by the addition of a THF solution (30.0 mL) of DPE–P3HT–DPE (M_n = 6200, PDI = 1.09, 0.059 g, 0.009 52 mmol (0.0190 mmol for DPE units)). After 6 h, degassed methanol was added, and the solution was poured into a large amount of methanol (100 mL) to precipitate the polymer. Isolated yield after Soxhlet extraction: 0.220 g (88%). M_n (GPC-RALLS) = 26 300, M_n (¹H NMR) = 26 100, PDI = 1.15.

Measurements. Molecular weights (MWs) and PDIs were measured by GPC on a Jasco GULLIVER 1500 equipped with a pump, an absorbance detector (UV, λ = 254 nm), and three polystyrene gel columns based on a conventional calibration curve using polystyrene standards. Chloroform was used as a carrier solvent at a flow rate of 1.0 mL/min at room temperature. Absolute molecular weights were measured with a HPLC system equipped with a pump, refractometer (RI), absorbance detector (UV, λ = 254 nm), online right-angle laser light scattering (RALLS) detector (λ = 670 nm), sample processor, and polystyrene gel columns connected in the following series: 650, 200, and 75 Å. THF was used as a carrier solvent at a flow rate of 1.0 mL/min at room temperature. ¹H NMR was recorded on a Bruker DPX (300 MHz) in chloroform-*d* calibrated to tetramethylsilane as an internal standard (δ H 0.00). Matrix-assisted laser desorption/ionization time-of-flight (MALDI-TOF) mass spectra were recorded on a Shimadzu AXMA-CFR mass spectrometer. The spectrometer was equipped with a nitrogen laser (337 nm) and with pulsed ion extraction. The operation was performed at an accelerating potential of 20 kV by linear-positive ion mode. Dithranol was used as a matrix. Mass values were calibrated by the three-point method with insulin plus H⁺ at m/z 5734.62, insulin β plus H⁺ at m/z 3497.96, and α -cyanohydroxycinnamic acid dimer plus H⁺ at m/z 379.35. DSC was performed with a Seiko EXSTAR 6000 DSC 6200. The samples were heated at 20 °C/min under nitrogen, and the second thermograms were recorded. Calibrations were made using indium as a standard. TGA was performed on a Seiko EXSTAR 6000 TG/DTA 6300 thermal analyzer at a heating rate of 10 °C/min. UV–vis absorption spectra of a polymer solution in chloroform and a thin film were recorded on a Jasco FP-750 spectrometer over a wavelength range of 250–800 nm. AFM phase images were taken with a SII-NT SPA 400 operating in a tapping mode. TEM images were obtained using a JEOL JEM-1010BS operated at 80 kV accelerating voltage. Block copolymer thin films were prepared by a drop-casting onto a carbon-coated TEM copper grid from a toluene solution (0.04 wt %), followed by solvent annealing with a toluene vapor at room temperature for 3 h. The films were then stained with a ruthenium oxide vapor for 10 min.

Results and Discussion

Living Anionic Polymerization of 4-Vinyltriphenylamine.

As mentioned in the Introduction, there were no reports on a living system to prepare low-polydisperse PVTPA having PDI < 1.1. Natori et al. improved the living system to some extent;¹⁰ however, highly reactive initiator, *tert*-BuLi, and the additive, TMEDA, must be employed to realize a high- M_n PVTPA with low PDIs. In their system, tolyllithium, which was in situ generated by the proton subtraction reaction of toluene (solvent) with *tert*-BuLi in the presence of TMEDA, was the actual initiator. In contrast, we first utilize *tert*-butylbenzene as a solvent which does not have acidic benzyl protons like toluene so that the actual initiator remains to be an alkylolithium. In addition, a polar solvent of THF was tried to use at –78 °C. There have never been examples to conduct such low temperature for the THF solvent in the polymerization of VTPA.

At first, the polymerization of VTPA was carried out in *tert*-butylbenzene at room temperature for 24 h, initiated with *sec*-BuLi under a high vacuum (10^{-6} Torr) condition (Scheme 1). On adding of a monomer solution to *sec*-BuLi, the solution immediately became brown-red, indicating the generation of a carbanion. The color remained unchanged until quenched with degassed methanol. The polymer yields were always more than 99%, as determined by ¹H NMR (runs 1–5). The results are summarized in Table 1. The GPC curves of PVTPA (Figure 1) show that the top peak shifts to a

Scheme 1. Living Anionic Polymerization of 4-Vinyltriphenylamine

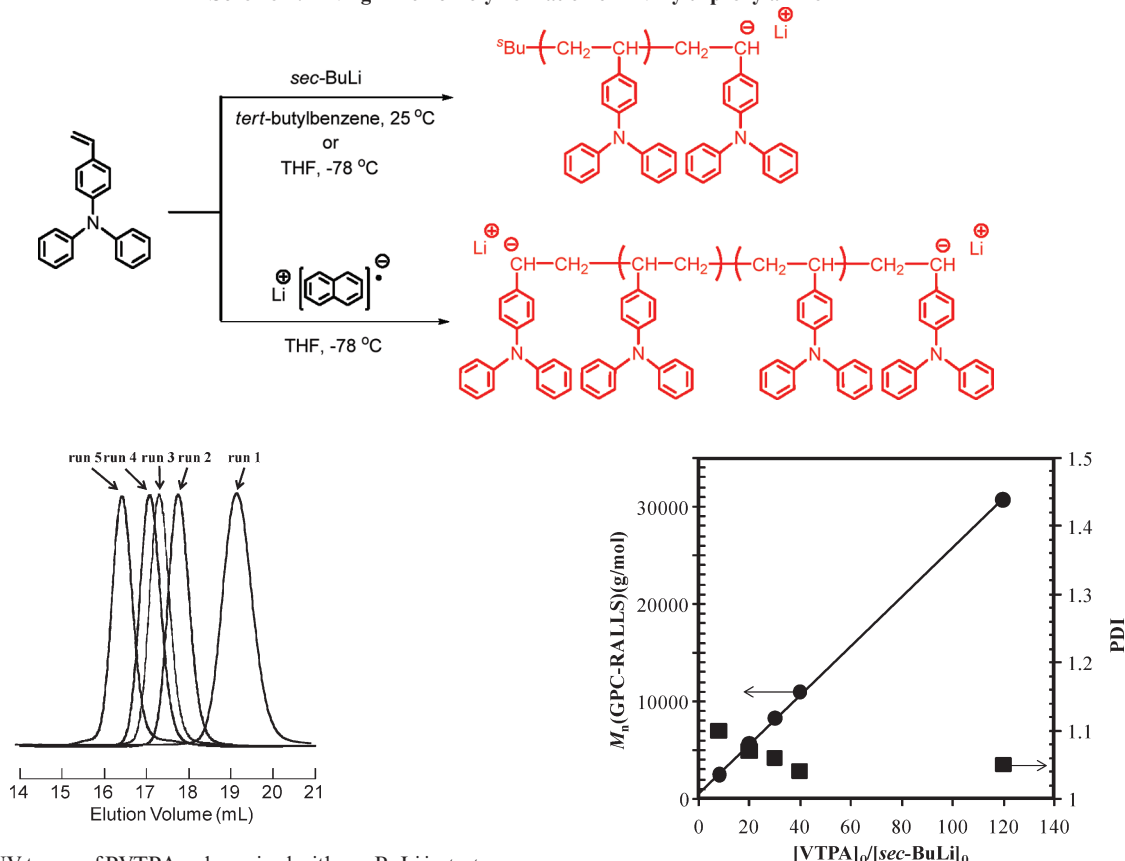


Figure 1. GPC UV traces of PVTPA polymerized with *sec*-BuLi in *tert*-butylbenzene at 25 °C for 24 h.

Table 1. Living Anionic Polymerization of 4-Vinyltriphenylamine in *tert*-Butylbenzene^a

run	initiator	condition	DP _n ^b	M _n (g/mol)			PDI
				calcd ^b	GPC-RALLS	¹ H NMR ^c	
1	<i>sec</i> -BuLi	25 °C	8	2 230	2 500	2 480	1.10
2	<i>sec</i> -BuLi	25 °C	20	5 490	5 670	5 440	1.07
3	<i>sec</i> -BuLi	25 °C	30	8 200	8 300	8 250	1.06
4	<i>sec</i> -BuLi	25 °C	40	10 900	11 000	10 300	1.04
5	<i>sec</i> -BuLi	25 °C	120	32 600	30 800	32 800	1.05
6	<i>sec</i> -BuLi	-78 °C	120	32 600	34 000	33 900	1.05
7	Li-Naph	-78 °C ^d	120	32 600	33 500	33 000	1.08

^a The yields of polymers are always more than 99%. ^b Calculated from the feed ratio of the initiator and monomer. ^c Calculated from the signal intensities assignable to six methyl protons of the *sec*-butyl group (0.6–0.8 ppm) and aromatic protons of the main chains (6.4–7.2 ppm).

^d The polymerization was carried out in THF.

higher molecular weight region by increasing the feed ratio of monomer to initiator while keeping symmetrical and very narrow distribution. The M_n values determined by GPC-RALLS and ¹H NMR agreed well with those calculated based on the feed ratio (Table 1). Figure 2 shows the feed-ratio ([VTPA]₀/[*sec*-BuLi]₀) dependence on the M_n value and PDI. The M_n values proportionally increase by increasing the feed ratio and the PDIs stay at less than 1.1. The representative MALDI-TOF mass spectra of PVTPA are shown in Figure 3 (run 3). Only a single series of signals with intervals corresponding to the monomer unit ($m/z = 271.36$) is found, assigning the α - and ω -ends to the butyl and proton groups, respectively. For instance, the 30-mer of PVTPA is observed at $m/z = 8198.0$, which is consistent with the theoretical value ($m/z = 8198.9 = 57.1$ (*sec*-Bu-) + 271.36 (monomer unit) \times 30 (degree of polymerization) + 1.0 (H)).

Figure 2. Plots of [VTPA]₀/[*sec*-BuLi]₀ vs M_n and PDI (circle and square indicate M_n (g/mol) and PDI, respectively, determined by GPC-RALLS).

Thus, it is obvious that the polymerization is initiated quantitatively with *sec*-BuLi, and no chain transfer is observed at all. In THF at -78 °C, similar successful polymerization results were obtained (run 6). In addition, Li-Naph instead of *sec*-BuLi could also be effective to initiate VTPA polymerization, affording low-PDI PVTPA with difunctional carbanions (run 7, Scheme 1). Consequently, we succeeded in synthesizing well-defined PVTPA with predictable M_n values and quite low PDIs (< 1.1) in all runs based on living anionic polymerization under the employed conditions. This success is thought to be derived from optimized conditions of the polymerization solution, where the inert solvent of *tert*-butylbenzene at room temperature or THF at -78 °C is first employed, to achieve the effective initiation simply from *sec*-BuLi and the polymerization without chain transfer and termination.

Synthesis of PVTPA-*b*-PMMA and PS-*b*-PVTPA-*b*-PS. Living anionic polymerization of VTPA initiated with *sec*-BuLi or Li-Naph was demonstrated in the preceding section. To corroborate the living nature of PVTPA chain end(s), we intended to synthesize a new series of block copolymers, PVTPA-*b*-PMMA and PS-*b*-PVTPA-*b*-PS, initiated with *sec*-BuLi and Li-Naph, respectively. The synthetic routes are depicted in Scheme 2.

First, *sec*-BuLi-initiated living PVTPA was end-capped with DPE in THF at -78 °C for 1 h. The red color of the living PVTPA solution turned immediately into dark red after adding DPE, suggesting the generation of 1,1-diphenylalkyl anions. After a 5-fold excess of LiCl was added to the carbanion, MMA was charged at once with vigorous stirring set at 700 rpm. The polymerization of MMA was

conducted in THF at $-78\text{ }^{\circ}\text{C}$ for 30 min. The results are summarized in Table 2. The GPC UV traces (Figure 4a)

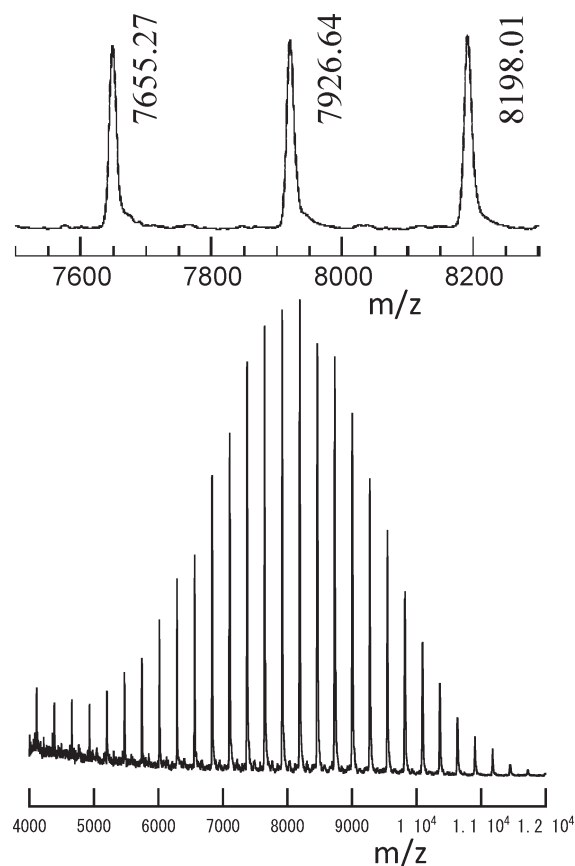


Figure 3. MALDI-TOF mass spectra of PVTTPA polymerized with *sec*-BuLi in *tert*-butylbenzene at $25\text{ }^{\circ}\text{C}$ for 24 h (run 3).

show the complete shift of the top peak of the PVTTPA precursor to a lower elution volume region while maintaining very low PDI after adding the second monomer. No deactivated PVTTPA was observed in the GPC traces which probed the living nature of PVTTPA. Agreement between the observed and calculated M_n values of PVTTPA-*b*-PMMA is excellent (Table 2). The PDI is extremely low (1.04). The ^1H NMR spectrum of PVTTPA-*b*-PMMA (Figure 5) shows the characteristic signals for both the PVTTPA and PMMA main chains with reasonable intensity. The composition determined by the same ^1H NMR spectrum is consistent with that calculated based on the feed ratio. Thus, the expected PVTTPA-*b*-PMMA could be synthesized without difficulty.

Next, a difunctional living PVTTPA initiated with Li-Naph was used for the crossover to styrene as the second monomer to synthesize an ABA triblock copolymer, PS-*b*-PVTTPA-*b*-PS. The results are also summarized in Table 2, and Figure 4b shows the GPC UV traces before and after the addition of styrene. The living nature of the difunctional PVTTPA as well as the structural homogeneity of PS-*b*-PVTTPA-*b*-PS were confirmed by GPC and ^1H NMR. It should be mentioned that the lithiated chain end(s) of PVTTPA is/are virtually living in THF at $-78\text{ }^{\circ}\text{C}$ and nucleophilic enough to either react with DPE or initiate the polymerization of styrene.

Synthesis of PVTTPA-*b*-P3HT-*b*-PVTTPA. As mentioned in the Introduction, regioregular P3HT is a high-performance material with high charge mobility and high solubility. PVTTPA has also been utilized for OLEDs due to its great hole-transporting property.^{1,2} The combination of PVTTPA and P3HT in a hybrid system may display a good hole-transporting performance. Unfortunately, there is no example of block copolymers containing both segments. Therefore, we were motivated to synthesize a novel coil-rod-coil triblock copolymer, PVTTPA-*b*-P3HT-*b*-PVTTPA. The synthetic routes are shown in Scheme 3.

Scheme 2. Synthesis of PVTTPA-*b*-PMMA and PS-*b*-PVTTPA-*b*-PS

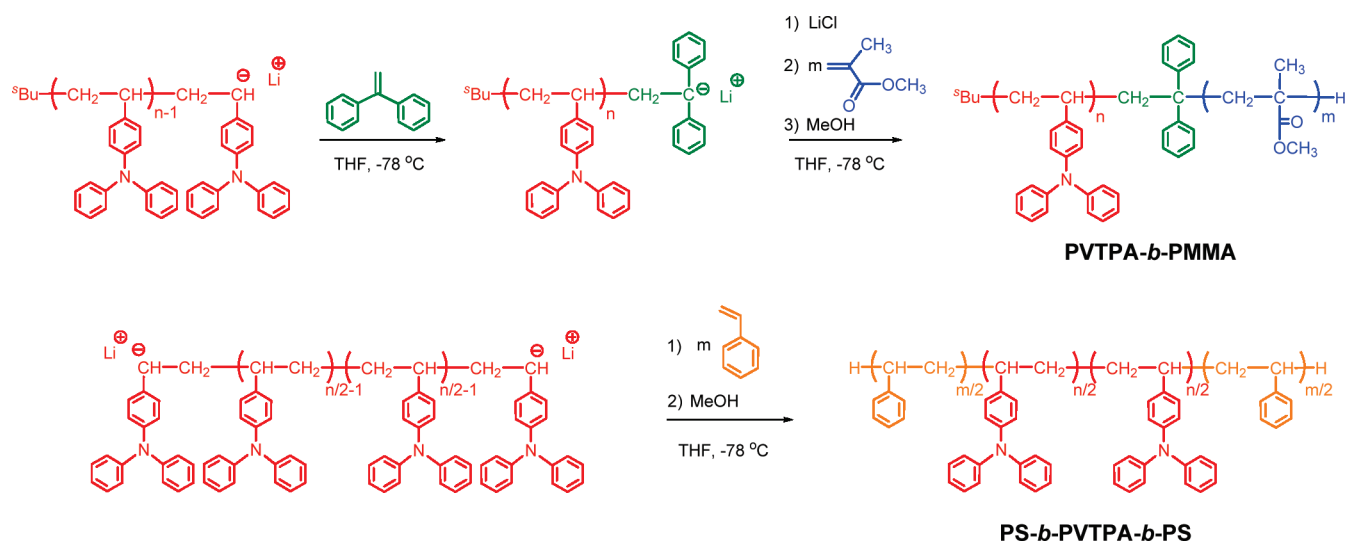


Table 2. Synthesis of PVTTPA-*b*-PMMA and PS-*b*-PVTTPA-*b*-PS in THF at $-78\text{ }^{\circ}\text{C}$ ^a

run	type	M_n (g/mol)				PVTTPA composition (wt %)	
		calcd ^b	GPC-RALLS	^1H NMR ^c	PDI	calcd ^b	^1H NMR
8	PVTTPA- <i>b</i> -PMMA	24 900	24 000	25 500	1.04	39	38
9	PS- <i>b</i> -PVTTPA- <i>b</i> -PS	38 700	38 000	38 600	1.07	48	48

^a The yields of polymers are always more than 99%. ^b Calculated from the feed ratio of the initiator and monomer. ^c Calculated from an M_n value of precursor PVTTPA determined by GPC-RALLS and the composition of a block copolymer determined by ^1H NMR.

The synthetic approach follows our previous methodology involving the linking reaction of polystyryllithium with DPE–P3HT–DPE.²⁶ A living PVTPA ($M_n = 10\,000$, PDI = 1.05) was first prepared with *sec*-BuLi in THF at $-78\text{ }^\circ\text{C}$ for 12 h, and then a dry THF solution of prepurified DPE–P3HT–DPE ($M_n = 6200$, PDI = 1.09, DPE functionality = 95%) was added ($[\text{living PVTPA}]/[\text{DPE unit}] = 2$). The color changed immediately into dark red, indicating the existence of 1,1-diphenylalkyl anions, and was maintained as such until quenched with degassed methanol after 6 h (run 10). The results are summarized in Table 3. The GPC curves are shown in Figure 6.

As shown in Figure 6a,b, each precursory homo-PVTPA and homo-P3HT shows a monomodal, symmetrical, and sharp peak. After the linking reaction, their peak tops shift to a higher molecular weight region (Figure 6c). The residual homo-PVTPA used in excess was successfully eliminated by Soxhlet extraction using ethyl acetate. The isolated PVTPA-*b*-P3HT-*b*-PVTPA possesses a major sharp peak with a very minor shoulder for a high-molecular-weight byproduct (< 5%) which cannot be identified (Figure 6d). The M_n values of PVTPA-*b*-P3HT-*b*-PVTPA determined by GPC-RALLS (26 300) and ^1H NMR (26 100) are in good

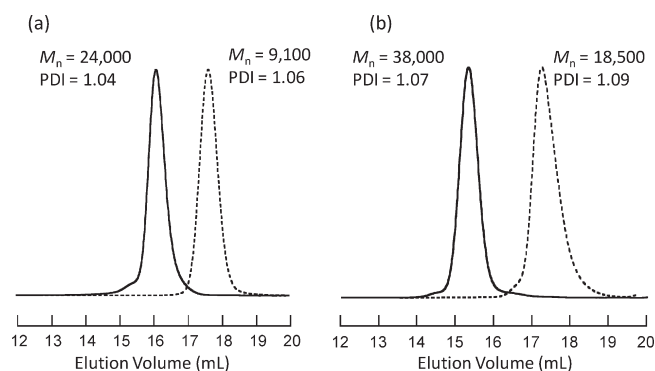


Figure 4. GPC UV traces of (a) PVTPA-*b*-PMMA (solid line) and precursor PVTPA (dashed line) and (b) PS-*b*-PVTPA-*b*-PS (solid line) and precursor PVTPA (dashed line).

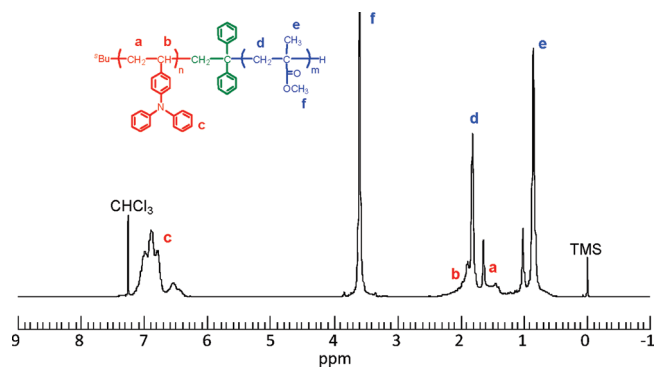


Figure 5. ^1H NMR spectrum of PVTPA-*b*-PMMA.

agreement with the calculated one (26 200). The PDI determined by GPC is low (1.15). In addition, ^1H NMR spectroscopy of PVTPA-*b*-P3HT-*b*-PVTPA confirmed the absence of the signal for the vinyl protons of the DPE moieties at 5.43 ppm, and the composition of two segments is almost consistent with that targeted (Figure 7, Table 3). Thus, the expected PVTPA-*b*-P3HT-*b*-PVTPA ($M_n = 10\,000$ –6200–10 000) could be successfully synthesized. Similarly, PVTPA-*b*-P3HT-*b*-PVTPA with the increased P3HT composition (run 11, $M_n = 8480$ –10 000–8480, PDI = 1.17) could also be synthesized (Table 3).

Thermal and Optical Properties of PVTPA-*b*-P3HT-*b*-PVTPA. The thermal property of the isolated PVTPA-*b*-P3HT-*b*-PVTPA (run 11) was investigated by DSC and TGA. The DSC thermograms of homo-PVTPA and PVTPA-*b*-P3HT-*b*-PVTPA are shown in Figure 8. The glass transition temperature (T_g) value of PVTPA is $148.5\text{ }^\circ\text{C}$. On the other hand, PVTPA-*b*-P3HT-*b*-PVTPA exhibits both T_g at $147.0\text{ }^\circ\text{C}$ and T_m at $231.1\text{ }^\circ\text{C}$, which correspond to the PVTPA and P3HT segments, respectively. This result supports the phase segregation of each domain of PVTPA-*b*-P3HT-*b*-PVTPA. Figure 9 shows the TG curve of PVTPA-*b*-P3HT-*b*-PVTPA. The sample shows high thermal stability ($T_{d,5\%} = 390\text{ }^\circ\text{C}$). Moreover, two-stage weight-loss behavior is observed from 390 to $450\text{ }^\circ\text{C}$ and above $450\text{ }^\circ\text{C}$. The first one is due to the degradation of PVTPA segments, whereas the second one is attributed to the decomposition of the P3HT segments, as expected for block formation.

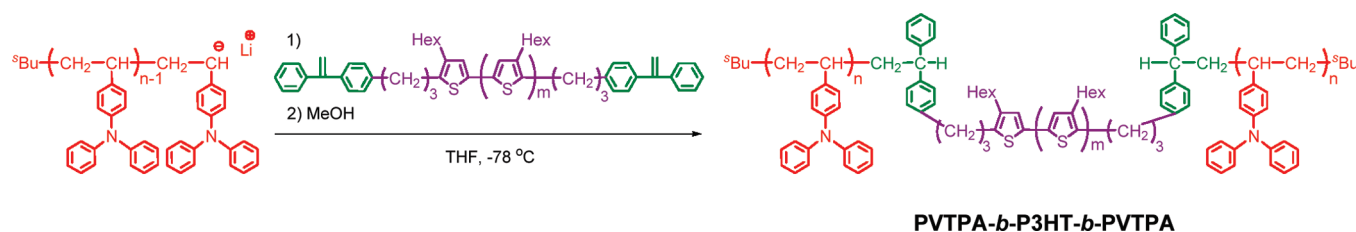
The optical property of PVTPA-*b*-P3HT-*b*-PVTPA (run 11) was studied by UV–vis (Figure 10) spectroscopy. As shown in Figure 10, the solution-state UV–vis spectrum of PVTPA-*b*-P3HT-*b*-PVTPA shows maximum absorptions (λ_{max} s) for the π – π^* transitions at 305 and 448 nm, corresponding to the PVTPA and P3HT segments, respectively (red line). In the film state, after solvent annealing with toluene, the λ_{max} at 448 nm for P3HT bathochromically shifts to a longer wavelength (560 nm) while maintaining the other λ_{max} at 305 nm for PVTPA. The film also shows a shoulder at around 608 nm related to vibronic absorption (purple line), similar to pristine P3HT film (green line). It is obvious that the amorphous PVTPA covalently connected to P3HT does not interfere with the high ordering behavior of P3HT where the PVTPA-rich

Table 3. Synthesis of PVTPA-*b*-P3HT-*b*-PVTPA in THF at $-78\text{ }^\circ\text{C}$ ^a

run	M_n (g/mol)				P3HT composition (wt %)	
	calcd ^b	GPC-RALLS	^1H NMR ^c	PDI	calcd ^b	^1H NMR
10	26 200	26 300	26 100	1.15	24	24
11	27 000	26 600	27 000	1.17	37	37

^a The yields of polymers are always more than 99%. ^b Calculated from the feed ratio of the initiator and monomer. ^c Calculated from an M_n value of precursor PVTPA determined by GPC-RALLS and the composition of a block copolymer determined by ^1H NMR.

Scheme 3. Synthesis of PVTPA-*b*-P3HT-*b*-PVTPA



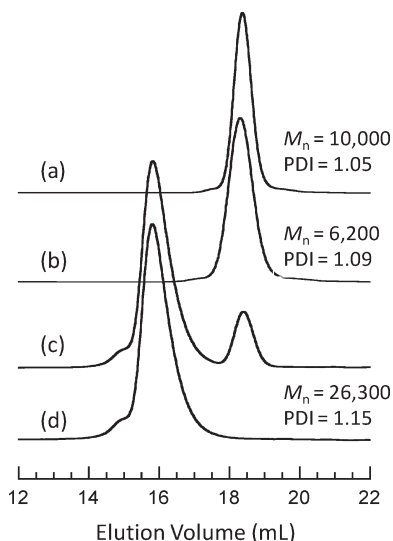


Figure 6. GPC traces of (a) precursor PVTPA, (b) precursor P3HT, (c) crude product, and (d) isolated PVTPA-*b*-P3HT-*b*-PVTPA (run 10).

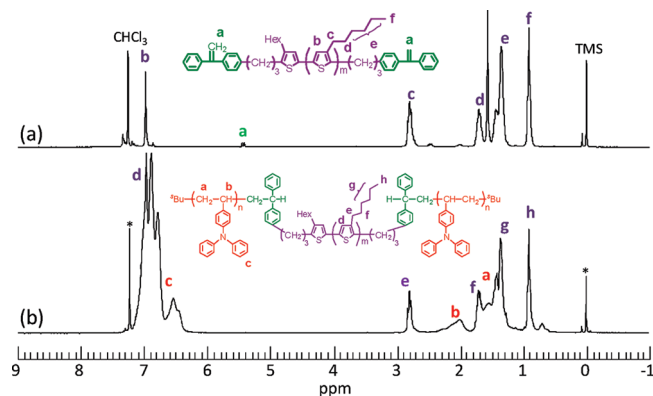


Figure 7. ^1H NMR spectra of (a) DPE-P3HT-DPE and (b) PVTPA-*b*-P3HT-*b*-PVTPA (run 10).

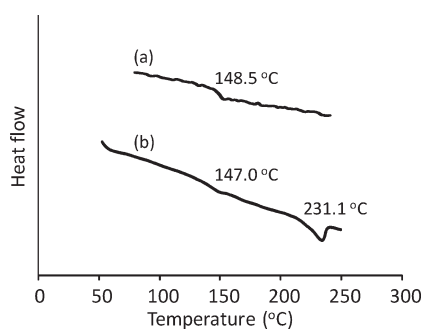


Figure 8. DSC thermograms of (a) precursor PVTPA and (b) PVTPA-*b*-P3HT-*b*-PVTPA (run 11).

and P3HT-rich domains are phase-separated. Unfortunately, in the case of the film treated by thermal annealing at 240 °C, the shoulder at 608 nm was decreased, which means less P3HT ordering structures (see blue line in Figure 10). We found that the difference in UV-vis absorptions was correlated to that in surface morphologies observed by AFM discussed afterward.

Self-Assemble Behavior of PVTPA-*b*-P3HT-*b*-PVTPA. To gain insight into the surface morphology, a thin film of

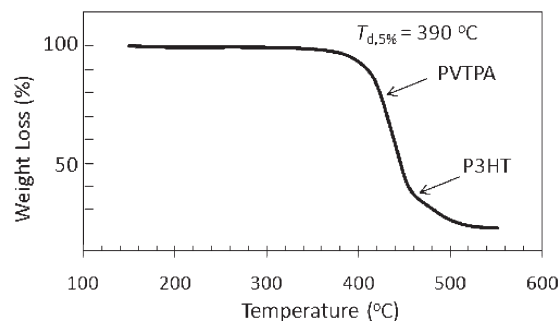


Figure 9. TG curve of PVTPA-*b*-P3HT-*b*-PVTPA (run 11).

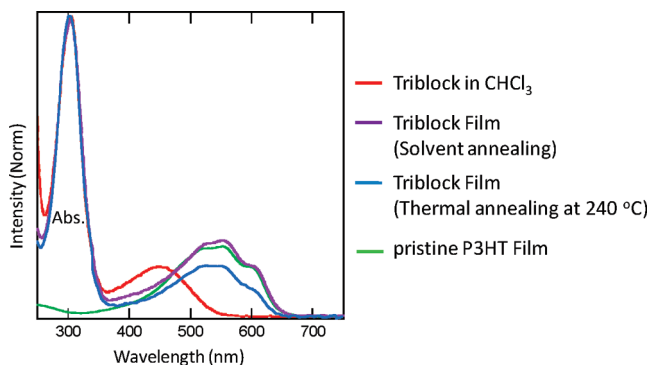


Figure 10. UV-vis spectra of PVTPA-*b*-P3HT-*b*-PVTPA (run 11) in CHCl_3 (red line), in the film state after solvent annealing with toluene (purple line) and thermal annealing at 240 °C for 12 h (blue line), and pristine P3HT film (green line).

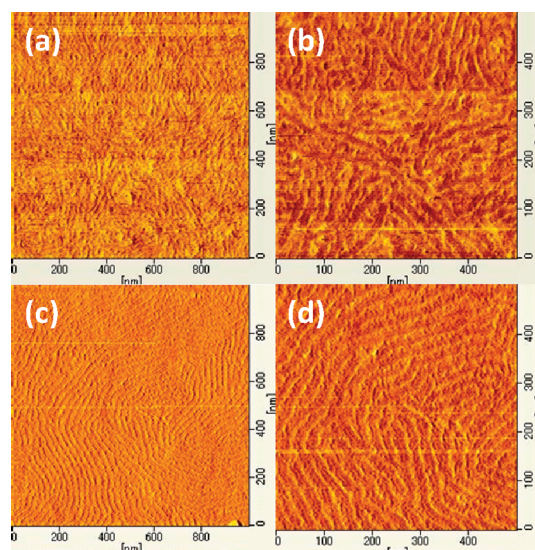


Figure 11. Tapping-mode AFM phase images of PVTPA-*b*-P3HT-*b*-PVTPA (run 11) thin film, (a, b) after thermal annealing at 240 °C for 12 h, (c, d) after solvent annealing (toluene) at room temperature for 3 h.

PVTPA-*b*-P3HT-*b*-PVTPA (run 11; P3HT: 37 wt %) was prepared by drop-casting from a toluene solution at room temperature, followed by thermal annealing at 240 °C (above the melting point of P3HT¹⁷) for 12 h under vacuum. The surface morphology of the cast film onto a mica was observed by AFM in a tapping mode (Figure 11a,b). Although nanofibril structures are observed with 12–15 nm widths where the bright and dark areas probably correspond to stiff-rod P3HT rich and flexible-coil PVTPA rich domains, respectively, there is little ordering texture in their

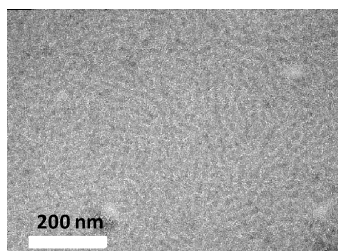


Figure 12. TEM image of PVTPA-*b*-P3HT-*b*-PVTPA (run 11) thin film after solvent annealing (toluene) at room temperature for 3 h.

morphology. A similar texture was also obtained in the film surface after thermal annealing at 150 °C. In contrast, when the cast film was treated by solvent annealing under exposure of a toluene vapor at room temperature for 3 h, a neat, uniform, and periodic morphology emerged over a large area, in which each phase-separated domain with 12–15 nm widths was well-connected through some micrometer lengths (Figure 11c,d). These periodic self-assemble structures may possibly be derived from the well-defined structure of PVTPA-*b*-P3HT-*b*-PVTPA with low PDI. PVTPA-*b*-P3HT-*b*-PVTPA with different composition (run 10; P3HT: 24 wt %) also shows a similar self-assemble behavior. To confirm the nanostructure, a TEM image of the sample film (run 11; P3HT: 37 wt %) treated by solvent annealing with toluene was taken (Figure 12). We could see the similar nanofibril morphology as AFM images, emerging with 12–15 nm widths, although the contrast is not very high (Figure 11c,d).

Conclusions

A living anionic polymerization of VTPA in *tert*-butylbenzene at 25 °C or THF at −78 °C initiated with *sec*-BuLi has been developed. The difunctional living PVTPA was also obtained by Li-Naph initiation. All the resulting PVTPA possess reasonably high- $M_{n,s}$ (~30K) and very low PDIs (1.04–1.10). In addition, a new series of PS-*b*-PVTPA-*b*-PS and PVTPA-*b*-PMMA were synthesized by sequential living anionic polymerization of different monomers. On the basis of these successful results, PVTPA-*b*-P3HT-*b*-PVTPA could be synthesized by the linking reaction of living PVTPA with DPE-P3HT-DPE. The low degree of structural heterogeneity of block copolymers was confirmed by GPC-RALLS and ^1H NMR. The thermal and optical properties of PVTPA-*b*-P3HT-*b*-PVTPA were investigated by DSC, TGA, and UV-vis spectroscopy. In addition, AFM and TEM images of a PVTPA-*b*-P3HT-*b*-PVTPA thin film treated by solvent annealing showed a periodic nanofibril phase-separated morphology with 12–15 nm widths and some micrometer lengths. The photovoltaic cell application based on PVTPA-*b*-P3HT-*b*-PVTPA as a novel p-type semiconductor is now under investigation. Especially, PVTPA domains of PVTPA-*b*-P3HT-*b*-PVTPA are expected to contribute with more efficient charge transportation rather than P3HT-based blocks containing insulators such as PS and PMMA.

Acknowledgment. We thank the Japan Society for the Promotion of Science (JSPS) for supporting this work by KAKENHI (20850014). We also thank Professor Akira Hirao for his helpful advice on living anionic polymerization of VTPA. The technical support of Mr. Ryohei Kikuchi, Center for Advanced Materials Analysis, Tokyo Institute of Technology, on the TEM operation is gratefully acknowledged.

References and Notes

- (1) Deng, L.; Furuta, P. T.; Garon, S.; Li, J.; Kavulak, D.; Thompson, M. E.; Fréchet, J. M. J. *Chem. Mater.* **2006**, *18*, 386.
- (2) Yeh, K.-M.; Lee, C.-C.; Chen, Y. *Synth. Met.* **2008**, *158*, 565.
- (3) Feast, W. J.; Peace, R. J.; Sage, I. C.; Wood, E. L. *Polym. Bull.* **1999**, *42*, 167.
- (4) Tew, G. N.; Pralle, M. U.; Stupp, S. I. *Angew. Chem., Int. Ed.* **2000**, *39*, 517.
- (5) Behl, M.; Hattemer, E.; Brehmer, M.; Zentel, R. *Macromol. Chem. Phys.* **2002**, *203*, 503.
- (6) Lindner, S. M.; Thelakkat, M. *Macromolecules* **2004**, *37*, 8832.
- (7) Tsutsumi, N.; Murano, T.; Sakai, W. *Macromolecules* **2005**, *38*, 7521.
- (8) Lindner, S. M.; Thelakkat, M. *Macromol. Chem. Phys.* **2006**, *207*, 2084.
- (9) Se, K.; Kijima, M.; Fujimoto, T. *Polym. J.* **1988**, *20*, 791.
- (10) Natori, I.; Natori, S.; Usui, H.; Sato, H. *Macromolecules* **2008**, *41*, 3852.
- (11) Di, C.-A.; Yu, C.; Liu, Y.-Q.; Zhu, D.-B. *J. Phys. Chem. B* **2007**, *111*, 14083.
- (12) (a) Kim, J. Y.; Lee, K.; Coates, N. E.; Moses, D.; Nguyen, T.-Q.; Dante, M.; Heeger, A. J. *Science* **2007**, *317*, 222. (b) Thompson, B. C.; Fréchet, J. M. J. *Angew. Chem., Int. Ed.* **2008**, *47*, 58. (c) Wei, Q.; Nishizawa, T.; Tajima, K.; Hashimoto, K. *Adv. Mater.* **2008**, *20*, 1.
- (13) Iovu, M. C.; Sheina, E. E.; Gil, R. R.; McCullough, R. D. *Macromolecules* **2005**, *38*, 8649.
- (14) Miyakoshi, R.; Yokoyama, A.; Yokozawa, T. *J. Am. Chem. Soc.* **2005**, *127*, 17542.
- (15) Yokozawa, T.; Adachi, I.; Miyakoshi, R.; Yokoyama, A. *High Perform. Polym.* **2007**, *19*, 684.
- (16) Ohshimizu, K.; Ueda, M. *Macromolecules* **2008**, *41*, 5289.
- (17) Zhang, Y.; Tajima, K.; Hirota, K.; Hashimoto, K. *J. Am. Chem. Soc.* **2008**, *130*, 7812.
- (18) Iovu, M. C.; Jeffries-El, M.; Sheina, E. E.; Cooper, J. R.; McCullough, R. D. *Polymer* **2005**, *46*, 8582.
- (19) Iovu, M. C.; Craley, C. R.; Jeffries-El, M.; Krankowski, A. B.; Zhang, R.; Kowalewski, T.; McCullough, R. D. *Macromolecules* **2007**, *40*, 4733.
- (20) Boudouris, B. W.; Frisbie, C. D.; Hillmyer, M. A. *Macromolecules* **2008**, *41*, 67.
- (21) Dai, C.-A.; Yen, W.-C.; Lee, Y.-H.; Ho, C.-C.; Su, W.-F. *J. Am. Chem. Soc.* **2007**, *129*, 11036.
- (22) Richard, F.; Brochon, C.; Leclerc, N.; Eckhardt, D.; Heiser, T.; Hadzioannou, G. *Macromol. Rapid Commun.* **2008**, *29*, 885.
- (23) Lee, J. U.; Cirpan, A.; Emrick, T.; Russell, T. P.; Jo, W. H. *J. Mater. Chem.* **2009**, *19*, 1483.
- (24) Sommer, M.; Lang, A. S.; Thelakkat, M. *Angew. Chem., Int. Ed.* **2008**, *47*, 7901.
- (25) Zhang, Q.; Cirpan, A.; Russell, T. P.; Emrick, T. *Macromolecules* **2009**, *42*, 1079.
- (26) Higashihara, T.; Ohshimizu, K.; Hirao, A.; Ueda, M. *Macromolecules* **2008**, *41*, 9505.
- (27) Higashihara, T.; Ueda, M. *React. Funct. Polym.* **2009**, *69*, 457.